

Measurement of the $^{197}\text{Au}(n,\gamma)$ cross section at n_TOF: towards a new standard

C. Massimi^{1,a}, U. Abbondanno², G. Aerts³, H. Álvarez⁴, F. Álvarez-Velarde⁵, S. Andriamonje³, J. Andrzejewski⁶, P. Assimakopoulos⁷, L. Audouin⁸, G. Badurek⁹, P. Baumann¹⁰, F. Bečvář¹¹, E. Berthoumieux³, F. Calviño¹², M. Calviani^{13,14}, D. Cano-Ott⁵, R. Capote^{15,16}, C. Carrapiço^{3,17}, P. Cennini¹⁸, V. Chepel¹⁹, E. Chiaveri¹⁸, N. Colonna²⁰, G. Cortes²¹, A. Couture²², J. Cox²², M. Dahlfors¹⁸, S. David⁸, I. Dillmann²³, C. Domingo-Pardo^{23,24}, W. Dridi³, I. Duran⁴, C. Eleftheriadis²⁵, M. Embid-Segura⁵, L. Ferrant^{†8}, A. Ferrari¹⁸, R. Ferreira-Marques¹⁹, K. Fujii², W. Furman²⁶, I. Goncalves¹⁹, E. González-Romero⁵, F. Gramegna¹³, C. Guerrero⁵, F. Gunsing³, B. Haas²⁷, R. Haight²⁸, M. Heil²³, A. Herrera-Martinez¹⁸, M. Igashira²⁹, E. Jericha⁹, F. Käppeler²³, Y. Kadi¹⁸, D. Karadimos⁷, D. Karamanis⁷, M. Kerveno¹⁰, P. Koehler³⁰, E. Kossionides³¹, M. Krčička¹¹, C. Lampoudis^{25,32}, H. Leeb⁹, A. Lindote¹⁹, I. Lopes¹⁹, M. Lozano¹⁶, S. Lukic¹⁰, J. Marganić⁶, S. Marrone²⁰, T. Martínez⁵, P. Mastinu³, A. Mengoni^{15,18}, P.M. Milazzo², C. Moreau², M. Mosconi²³, F. Neves¹⁹, H. Oberhammer⁹, S. O'Brien²², J. Pancin³, C. Papachristodoulou⁷, C. Papadopoulos³², C. Paradela⁴, N. Patronis⁷, A. Pavlik³³, P. Pavlopoulos³⁴, L. Perrot³, M.T. Pigni⁹, R. Plag²³, A. Plompen³⁵, A. Plukis³, A. Poch²¹, J. Praena¹³, C. Pretel²¹, J. Quesada¹⁶, T. Rauscher³⁶, R. Reifarth²⁸, C. Rubbia³⁷, G. Rudolf¹⁰, P. Rullhusen³⁵, J. Salgado¹⁷, C. Santos¹⁷, L. Sarchiapone¹⁸, I. Savvidis²⁵, C. Stephan⁸, G. Tagliente²⁰, J.L. Tain²⁴, L. Tassan-Got⁸, L. Tavora¹⁷, R. Terlizzi²⁰, G. Vannini¹, P. Vaz¹⁷, A. Ventura³⁸, D. Villamarin⁵, M.C. Vicente⁵, V. Vlachoudis¹⁸, R. Vlastou³², F. Voss²³, S. Walter²³, M. Wiescher²², and K. Wisshak²³

The n_TOF Collaboration (www.cern.ch/ntof)

¹Dipartimento di Fisica, Università di Bologna, and Sezione INFN di Bologna, Italy – ²Istituto Nazionale di Fisica Nucleare, Trieste, Italy – ³CEA/Saclay-DSM/DAPNIA, Gif-sur-Yvette, France – ⁴Universidad de Santiago de Compostela, Spain – ⁵Centro de Investigaciones Energeticas Medioambientales y Tecnológicas, Madrid, Spain – ⁶University of Lodz, Lodz, Poland – ⁷University of Ioannina, Greece – ⁸Centre National de la Recherche Scientifique/IN2P3-IPN, Orsay, France – ⁹Atominstytut der Österreichischen Universitäten, Technische Universität Wien, Austria – ¹⁰Centre National de la Recherche Scientifique/IN2P3-IRES, Strasbourg, France – ¹¹Charles University, Prague, Czech Republic – ¹²Universidad Politécnica de Madrid, Spain – ¹³Istituto Nazionale di Fisica Nucleare, Laboratori Nazionali di Legnaro, Italy – ¹⁴Dipartimento di Fisica, Università di Padova, Italy – ¹⁵International Atomic Energy Agency (IAEA), Nuclear Data Section, Vienna, Austria – ¹⁶Universidad de Sevilla, Spain – ¹⁷Instituto Tecnológico e Nuclear (ITN), Lisbon, Portugal – ¹⁸CERN, Geneva, Switzerland – ¹⁹LIP – Coimbra & Departamento de Física da Universidade de Coimbra, Portugal – ²⁰Istituto Nazionale di Fisica Nucleare, Bari, Italy – ²¹Universitat Politècnica de Catalunya, Barcelona, Spain – ²²University of Notre Dame, Notre Dame, USA – ²³Forschungszentrum Karlsruhe GmbH (FZK), Institut für Kernphysik, Germany – ²⁴Instituto de Física Corpuscular, CSIC-Universidad de Valencia, Spain – ²⁵Aristotle University of Thessaloniki, Greece – ²⁶Joint Institute for Nuclear Research, Frank Laboratory of Neutron Physics, Dubna, Russia – ²⁷Centre National de la Recherche Scientifique/IN2P3 – CENBG, Bordeaux, France – ²⁸Los Alamos National Laboratory, New Mexico, USA – ²⁹Tokyo Institute of Technology, Tokyo, Japan – ³⁰Oak Ridge National Laboratory, Physics Division, Oak Ridge, USA – ³¹NCSR, Athens, Greece – ³²National Technical University of Athens, Greece – ³³Institut für Isotopenforschung und Kernphysik, Universität Wien, Austria – ³⁴Pôle Universitaire Léonard de Vinci, Paris-La Défense, France – ³⁵CEC-JRC-IRMM, Geel, Belgium – ³⁶Department of Physics – University of Basel, Switzerland – ³⁷Università degli Studi Pavia, Pavia, Italy – ³⁸ENEA, Bologna, Italy

Abstract. Two different detectors and techniques are employed at n_TOF facility, at CERN, to improve the accuracy of the neutron capture cross section of $^{197}\text{Au}(n,\gamma)$: a total absorption calorimeter and a set of C_6D_6 . The accurate knowledge of this cross section is of great importance for all the (n,γ) reactions study. The neutron capture cross section and nuclear resonance parameters of the ^{197}Au have been measured in the energy range of 1 eV to 1 keV. The present work shows in average a good agreement with evaluated data libraries, although sizeable differences have been observed for some resonances. Two new resonances have also been discovered. The accuracy of the resonance partial widths has been improved and the main nuclear quantities such as the neutron strength function have been extracted.

1 Introduction

The main objectives of the experimental activity of the neutron time-of-flight facility, n_TOF, at CERN, are the accurate measurements of neutron capture cross sections related to nuclear astrophysics [1,2] and the collection of nuclear data related

to emerging nuclear technologies for energy production and nuclear waste transmutation [3,4]. The n_TOF facility, based on an idea by Rubbia et al. [5], became fully operational in May 2002, when the scientific program started. A detailed description of its performances can be found elsewhere [6]. The high instantaneous flux, the good energy resolution, and the low background that characterize the n_TOF neutron beam, associated with high-performance detectors and data acquisition

^a Presenting author, e-mail: massimi@bo.infn.it

systems, allow to perform accurate measurement of isotopically enriched samples, including radioactive isotopes.

Neutron capture cross sections are usually derived after normalization to a standard cross section that is accurately known. To this end, the first resonance at 4.9 eV of the $n + {}^{197}\text{Au}$ reaction can be utilized. In fact, the parameters of this resonance are known with an accuracy of 3%. In addition, the Au cross section is considered as a standard in the energy range above 200 keV, and measurements of capture cross sections rely on this information as well. High accuracy measurements of the capture cross section for Au have been performed at the n_TOF facility, with the aim of extending the energy range of the standard from 1 eV up to 10 keV, with two different detection systems: a set of two C_6D_6 detectors with extremely low neutron sensitivity, and a total absorption calorimeter based on BaF_2 scintillator crystals. In particular, this latter device yields excellent discrimination of ambient background and of competing reactions.

2 Experimental details

2.1 The n_TOF facility

At n_TOF, neutrons are generated via spallation by the 20 GeV/c protons from the CERN Proton Synchrotron (PS) accelerator complex impinging onto a massive target of natural lead. The measuring station is located at 187.5 m from the spallation target, inside the tunnel that houses the evacuated neutron flight path. Because of the prolific neutron production provided by spallation reactions and the very intense beam of 7×10^{12} protons/pulse, the instantaneous neutron flux at n_TOF is more than two order of magnitude higher than at the other existing facilities. Background due to charged particles and γ -rays originating from the spallation target is efficiently reduced by several meters of concrete and iron shieldings, a sweeping magnet, and a combination of two collimators. For capture measurements with a 1.9 cm diameter collimator beam spot, the instantaneous flux amounts to 10^5 neutrons/cm²/pulse for neutron energies between 0.1 eV and 20 GeV.

2.2 Capture setup

The neutron capture event is characterized by the deexcitation of the compound nucleus by emission of a γ -ray cascade. To detect the prompt capture γ -rays, at n_TOF we utilised two different techniques: the Pulse Height Weighting Technique (PHWT) with two C_6D_6 liquid scintillation detectors [10] and a total absorption calorimeter (TAC), a spherical 4π detector. The first solution is preferable when the total cross section is dominated by the elastic channel: the low neutron sensitivity of C_6D_6 allows to carry out measurements even when the ratio capture/scattering is extremely small. Instead when fission is in competition with capture reaction, or when the natural radioactivity of the sample is high, one needs to record the full electromagnetic cascade (TAC measurement) to distinguish the capture γ -rays from the background ones. Since $\text{Au}(n,\gamma)$ has been utilized, at n_TOF, for cross sections normalization, a large body of capture data for gold obtained with the two independent technique have been collected. The

Table 1. Au samples features for the two capture measurements.

	TAC	C_6D_6
Diameter (cm)	1.0	2.205
Weight (g)	0.1854	1.871
Thickness (cm)	1.22×10^{-2}	2.5×10^{-2}
Areal density (atoms/barn)	7.3×10^{-4}	1.498×10^{-3}

main characteristics of the capture study with the PHWT have been published [11]. Here we concentrate on the TAC analysis. The neutron capture detection system consists in a segmented total absorption calorimeter made of 40 BaF_2 scintillation crystals. The TAC has nearly 100% detection efficiency for electromagnetic cascade and a good energy resolution (15% at 662 keV and 6% at 6.1 MeV) in the energy range of interest. The Au sample (see table 1) is placed at the geometric center of the TAC and surrounded by a $\text{C}_{12}\text{H}_{20}\text{O}_4({}^6\text{Li})_2$ neutron absorber placed inside the inner space of the TAC. The neutron absorber reduce the number of scattered neutrons reaching the detector. The neutron flux is measured by a silicon monitor (SiMon) [8] consisting of a thin ${}^6\text{Li}$ deposit on a thin Mylar foil surrounded by a set of four silicon detectors outside the neutron beam for recording the tritons and α particles from the ${}^6\text{Li}(n,\alpha){}^3\text{H}$ reaction. The Data Acquisition System (DAQ) used in the measurements consists of 54 channels of high performance flash ADCs [9]. Each channel has 8 Mbytes memory operating at a sampling rate of 500 Msamples/s, thus allowing to record the full detector history for neutron energy ranges above 0.3 eV. After zero suppression and data formatting, especially designed pulse shape analysis routines extract from the digitized detector signals the necessary information for the data analysis.

3 Data analysis

3.1 Determination of the capture yield

The capture yield $Y(E_n)$, which is the fraction of the number of neutrons $\Phi(E_n)$ with energy E_n incident on the sample and producing a capture event, can be determined in a simple way from the number of γ -cascades observed $N_{obs}(E_n)$. Without consideration of the background this is given by

$$Y(E_n) = \frac{N_{obs}}{\epsilon} \cdot \frac{1}{\Phi(E_n)}, \quad (1)$$

where ϵ is the TAC detection efficiency. It is independent of the neutron energy and depends on the analysis conditions, such as multiplicity (that is the number of BaF_2 crystals hit by a γ -ray) and cuts on energy deposition. The ratio between the yield obtained at n_TOF and that tabulated in literature, for the first $\text{Au}(n,\gamma)$ resonance, gives the normalization factor. This ratio results to be the product of the detection efficiency times the fraction of neutrons really impinging on the sample. In figure 1 the energy deposition for $\text{Au}(n,\gamma)$ measurement is shown, the Au capture peak at 6.5 MeV and the various components of the background can be identified. Indeed the scattered neutrons can be stopped in the ${}^{10}\text{B}$ -loaded carbon fiber capsules surrounding the crystals, or they can be captured

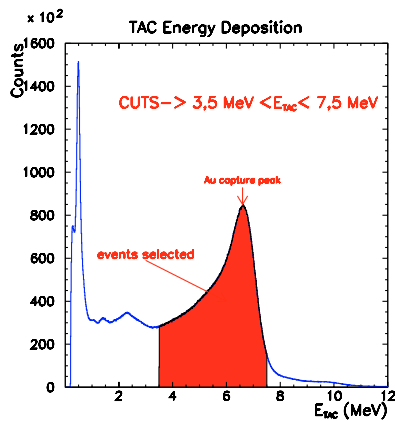


Fig. 1. Energy deposition for Au(n,γ) reaction. All events detected without conditions in energy deposition and multiplicity. For this analysis the conditions in energy depositions are: $3.5\text{ MeV} < E_{TAC} < 7.5\text{ MeV}$ to avoid background events.

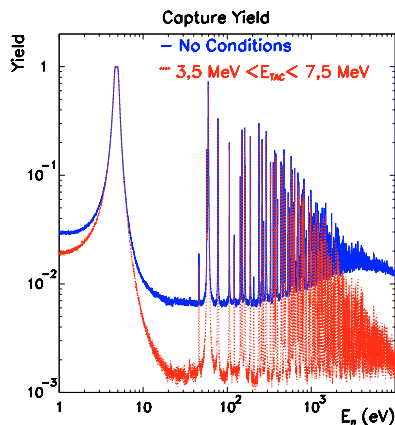


Fig. 2. Au capture yield extracted from the same data set with different conditions on energy deposition spectra, see figure 1.

by the Hydrogen present in the neutron absorber, giving rise to the 480 keV and 2.2 MeV γ -ray respectively. Finally, they can be captured inside by Ba inside the crystals, yielding a 9 MeV γ -cascade. Applying conditions on energy deposition spectra (see fig. 1) and/or in multiplicity we have minimized the background. This selection of the capture events lowers the detection efficiency down to 60%. The resulting yield is shown in figure 2.

3.2 Corrections

Although the data acquisition system used for this experiment in principle introduces only a negligible dead-time, the measurements indicated that a correction is needed to take into account the dead-time introduced by the calorimetric method. Indeed, in the analysis we are forced to set a time-window to identify a capture event (all γ -rays detected in this window are thought to belong to the same capture event). In this time-window there exist a probability of detecting two different capture events. Due to the constraints in the total γ -ray energy and in the multiplicity of the events, it may happen that events which are actually due to two or more captures can be lost or seen as one event (with slightly different E_{TAC} and multiplicity). This sort of “detector dead-time” can

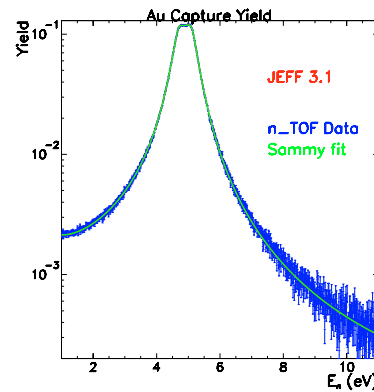


Fig. 3. SAMMY fit of the s -wave ^{197}Au resonance at 4.9 eV.

be corrected in the extraction of the yield by applying the following relation [12]:

$$C_r^R = \frac{C_r}{1 - C_r \times \Delta t} \quad (2)$$

where C_r^R is the real (true) counting rate, C_r is the registered counting rate and Δt is the dead-time (in our case, the coincidence window). A corresponding correction factor for the measured count rate was obtained as a function of TOF by means of the “paralyzable model” approximation, which accounts for the software dead time of 20 ns [12]. This correction is lower than 5%, which is reached at the top of the main resonances. Nevertheless, it affects the results of the resonance analysis, because of the distortions of the resonance shapes. Pile up may occur if signals are too close to be correctly identified by the reconstructions routine. Indeed the pulse shape algorithm may fail to find a signal in the tail of another one, because of the high counting rate. In this case Monte Carlo simulation are needed to estimate this effect. Most of the pile up, however, concerns γ -rays of low energy, below 200 keV, so that a minimization is obtained in the present analysis conditions, that is multiplicity greater than 2 and $3.5\text{ MeV} < E_{TAC} < 7.5\text{ MeV}$. We have estimated that the residual pile up effect is less than 1%. Neutrons scattered at the sample can be captured by the TAC materials (mainly in the Ba isotopes) and considered as true capture events. Such a background, also called neutron sensitivity of the detector, for Au(n,γ) is of the order of 2% only for resonance with particularly high Γ_n , and must be subtracted.

4 Results

In the Resolved Resonance Region (RRR) the capture cross section of ^{197}Au is expressed in terms of R-matrix resonance parameters calculated in the Reich-Moore approximation with the code SAMMY [13]. The fitting procedure consisted in the extraction of the resonance parameters from the measured capture yields. The fit to the resonances was performed in different ways in order to check the reliability of the extracted parameters. In general, the three resonance parameters, E_R , Γ_γ and Γ_n are left free to vary while the normalization factor, extracted from the first resonance, see figure 3, is kept fixed. The spin assignment of each level was taken from the ENDF-VII [14] or JEFF-3.1 [15] libraries or Mughabghab [16]

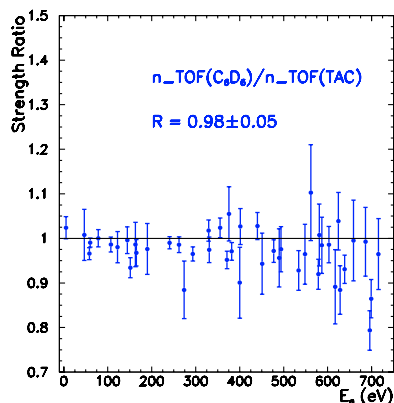


Fig. 4. The capture kernels of TAC data compared with C_6D_6 data. The agreement is better than 2%.

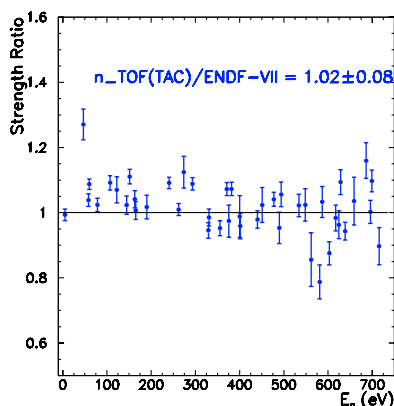


Fig. 5. Comparison with ENDF-VII, the newest cross section library (2006), in average very good.

evaluation. The parameters of 47 resonances (2 of them were identified for the first time) were extracted in the energy range between 1 and 720 eV. The parameters were used to calculate the capture kernels for each resonance, defined as $G(J) \cdot \Gamma_\gamma \cdot \Gamma_n / (\Gamma_n + \Gamma_\gamma)$, where $G(J)$ is the statistical spin factor. TAC data were compared with those of C_6D_6 , finding a good agreement, see figure 4. Since it was verified that both capture detection technique are consistent, the capture kernels of TAC n_TOF data were compared with those listed in ENDF-VII and JEFF-3.1 libraries and the previous data compiled by S.F. Mughabghab. Even though the capture kernel of some resonances present discrepancies, the whole set of data is in good agreement. Mainly, the discrepancies are present for the weaker resonances, probably not well measured in past measurements. An average difference of 1–2% was found, see for example figure 5 (2% with respect to ENDF-VII; 1% with respect to Mughabghab and –1% with respect to JEFF-3.1).

5 Discussion of uncertainties

The total uncertainty in the cross section consists of several contribution. The main source comes from the determination of the normalization constant, that is the product of the neutron beam interception factor (fraction of the neutron impinging on the sample) and the efficiency of the TAC. This constant is determined from the analysis of the first $Au(n,\gamma)$ resonance,

which has an uncertainty of 3%. An uncertainty of 2% is related to the shape of the neutron flux. Other contributions come from background subtraction, dead-time and pile up correction estimated around 1%. Adding up these components the overall uncertainty is around 3%. A covariance propagation for the present analysis procedure is still in progress.

6 Conclusions

The n_TOF measurement is an important step forward towards the extension of the $Au(n,\gamma)$ reaction as a standard in different energy regions, thanks to the high accuracy (due to low background and low neutron sensitivity) and resolution. The combined analysis of the BaF_2 TAC and the C_6D_6 detectors allowed to extract resonance parameter with an accuracy lower than 5%. The preliminary $Au(n,\gamma)$ analysis shows the potentiality of the TAC. Although good agreement with ENDF and/or JEFF is observed in average, discrepancies were found for some resonances in the energy region 200 eV–1 keV. Two new resonances were observed. The determination of resonance parameters is now in progress and we expect to extend this analysis up to 10 keV. A combined analysis with Au data from other facilities would improve the overall accuracy and would provide a strong impulse to define a new standard cross section of neutron capture on gold.

This work is part of the European Commission 5th Framework Programme project $N_TOF-AND-ADS$ under contract FIKW-CT-2000-00107.

References

1. G. Wallerstein et al., *Rev. Mod. Phys.* **69**, 995 (1997).
2. F. Käppeler, *Prog. Part. Nucl. Phys.* **43**, 419 (1999).
3. W. Gudowski, *Nucl. Phys. A* **722**, 485c (2003).
4. *Accelerator Driven System and Fast Reactors in Advanced Nuclear Fuel Cycle*, ISBN 92-64-18482-1 NEA-OEDC Report, 2002.
5. C. Rubbia et al., *Tech. Rep. CERN/LHC/98-02*, 1998.
6. U. Abbondanno et al., *Tech. Rep. CERN-SL-2002-053 ECT*, 2003.
7. S. Marrone et al., *Nucl. Instrum. Meth. A* **538**, 692 (2005).
8. S. Marrone et al., *Nucl. Instrum. Meth. A* **517**, 389 (2004).
9. <http://www.acqiris.com>.
10. R. Plag et al., *Nucl. Instrum. Meth. Phys. Res. A* **496**, 425 (2003).
11. To access n_TOF full paper list, visit the website: http://www.cern.ch/n_TOF.
12. G.F. Knoll, *Radiation Detection and Measurement*, 3rd edn. (John Wiley & Sons, 2000).
13. N.M. Larson, Oak Ridge National Laboratory, ORNL/TM-2000/252, 2000.
14. M.B. Chadwick, P. Oblozinsky et al. (CSEWG collaboration), *ENDF/B-VII: Next Generation Evaluated Nuclear Data Library for Nuclear Science and Technology*, *Nucl. Data Sheets* **107**, No. 12, 2931 (2006).
15. To access to neutron data evaluated and experimental, visit the website: <http://www.nndc.bnl.gov/index.jsp>.
16. S.F. Mughabghab, *Atlas of Neutron Resonances, Resonance Parameters and Thermal Cross Section Z = 1-100* (Elsevier Science, 2006).